ELSEVIER

Earth and Planetary Science Letters 121 (1994) 245–258

EPSL

Systematics of ridge propagation south of 30°S

Jason Phipps Morgan, David T. Sandwell

Institute of Geophysics and Planetary Physics, UCSD, La Jolla, CA 92093, USA

(Received March 29, 1993; revision accepted 5 November, 1993)

Abstract

New high-resolution Geosat altimetry data south of 30°S reveal numerous propagating ridge wakes along intermediate- and slow-spreading ridges. These new examples provide a large enough database to establish systematics of ridge propagation. Almost all active propagating ridges propagate down a regional along-axis gravity or bathymetry gradient. The sense of the propagating ridge offset (right lateral vs. left lateral) is related to recent changes in spreading direction. We find there is a significant difference between the propagation of ridges with an axial high morphology which propagate at greater than ~ 50% of their full-spreading rate and ridges with a median valley morphology which usually propagate at ~ 25% of their spreading rate. The axial high propagators leave behind an asymmetric wake; the outer pseudofault appears as a continuous linear trough/step while the sheared zone appears as a chain of small gravity bumps. While we clearly see the propagating ridge wakes from offsets greater than ~ 10 km at slow- and intermediate-spreading ridges, at ridges spreading faster than ~ 75 mm/yr the amplitude of the wake topography decreases to the point where we no longer see these wakes in Geosat altimetry data. The systematics seen in this new data set support a fracture mechanics model for the dynamics of ridge propagation.

1. Introduction

Our understanding of the dynamics of ridge propagation has been hindered by the small number of examples that have been explored by shipboard magnetic and bathymetric mapping. Most propagating ridges (PRs) were found by their effect on seafloor magnetic anomalies. Here we examine new high-resolution sea-surface free-air gravity data [1] which provide complete coverage of the mid-ocean ridge system south of 30°S. We find 28 examples of migrating ridge offsets and use this large sample to reliably explore some of the systematics of ridge propagation.

The data set that we use is the sea-surface gravity field of Sandwell and Smith [1] derived from Geosat, ERS-1 and Seasat satellite altimetry data. We use this data in two complementary forms. A color picture of the surface gravity field, suitably shaded (Plate 1), provides both long-wavelength and short-wavelength gravity information about the oceanic spreading center system. However, to optimally highlight each PR system requires two angles of illumination to enhance each of the arms of the V-shaped 'wake' left by a migrating ridge offset. Thus, for tectonic identification of short-wavelength structures it is useful apply an isotropic high-pass filter. We use the Laplacian operator to extract the vertical gravity gradient (or the sea-surface curvature $dg/d_z = d^2U/dz^2 = -[d^2U/dx^2 + d^2U/dy^2]$ since $\nabla^2 U =$

[MK]

SSDI 0012-821X(93)E0214-5

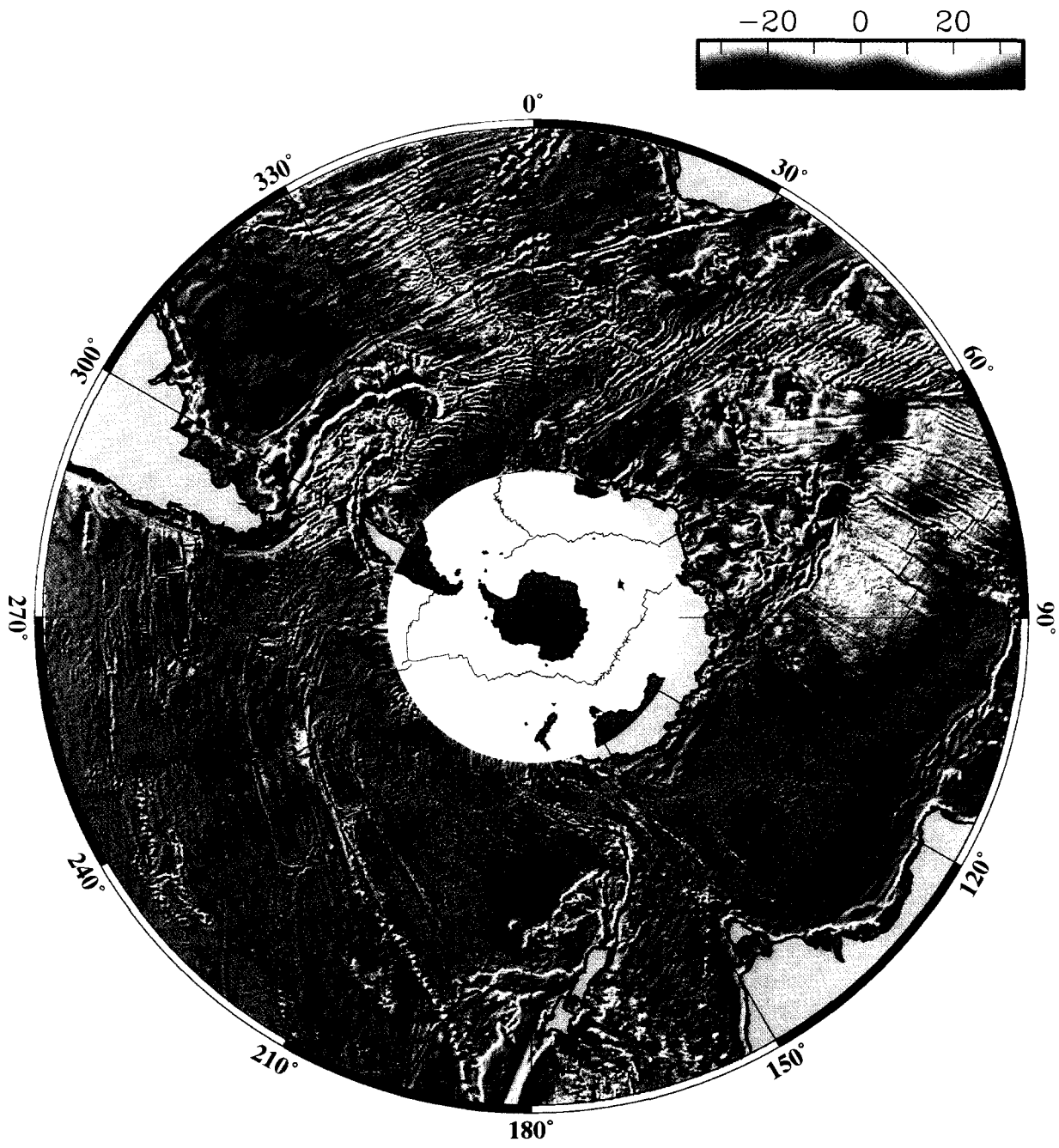

Plate 1. Global shaded relief map of the free-air gravity south of 30°S [1]. Trace of the global mid-ocean ridge system is shown by a light black line. Short-wavelength structure is enhanced by shading the gravity field with an illumination direction from the upper left corner of the page. Inset: Trace of the global mid-ocean ridge system is shown by a light black line. Near-ridge traces of active propagating ridge pseudofault 'wakes' noted in Table 1 are shown by red lines. See individual subpanels ein Fig. 1 for more details of propagating ridge structure.

0) as shown in Fig. 1. We find, through comparison with multibeam data along the Southeast Indian Ridge [2,3], that these maps (Plate 1 and Fig. 1) resolve major migrating ridge offsets (offsets larger than ~10 km). Thus this survey is likely to contain a complete record of the 'disturbed wake' left by all propagating ridges of this size; smaller features are likely to be less well sampled. Plate 1 and Fig. 1 show the locations of the 28 active propagating ridges that we find on the global ridge system south of 30°S. Several of these features have been seen in previous ship and aeromagnetic studies [2,4,5]. Table 1 is a compilation of the kinematic characteristics of these propagating ridges. It also shows the locations of six overlapping spreading center (OSC) offsets along the Pacific–Antarctic Ridge that we see in the Geosat data south of 30°S. Although we can see the offsets, we cannot determine the sense of migration from Geosat data alone. Lonsdale [6], with additional ship data, has determined the current migration direction of several of these OSCs. Table 2 is a compilation of the characteristics of previously mapped active propagating ridges. Note that Table 2 only includes other PR systems that are comparable in offset size and wake relief to those seen in this study. In particular, we make no attempt to compile systematics of migrating OSCs along the East Pacific Rise [7] and Pacific–Antarctic Rise [6], since their migration is not apparent in the Geosat data.

2. Characteristics of active propagating ridges

Several trends are evident from our gravity analysis of PRs (Fig. 1, Table 1 and Table 2):

(1) Most PRs are observed at intermediate- and slow-spreading ridges (33–75 mm/yr full rate). (Note, however, that the very slow spreading Southwest Indian Ridge shows no Geosat evidence of ridge propagation.) Fast-spreading ridges (i.e., Pacific–Antarctic Rise and Southern East Pacific Rise) do not show clear gravity expressions of PR wakes even where there is a clear expression of a non-transform offset such as an overlapping spreading center (OSC). Moreover, we do not see small active PRs (we prefer to call these migrating OSCs) that are apparent in a multibeam bathymetric survey of the Pacific–Antarctic Rise [6]. North of 30°S migrating OSCs have been seen in ship surveys of very fast spreading ridges (e.g., the 20°S migrating OSC along the East Pacific Rise [8]). Our inability to observe PRs at higher spreading suggests that their gravity amplitude is less than the noise in the Geosat-derived gravity field (~5 mGal). The 25°S Easter PR (#39) is also migrating faster than the observed Geosat PR/OSC transition and appears to be a typical propagating ridge in many respects [9,10], although it has a larger offset than the migrating OSCs south of 30°S.

(2) Most PRs seen in Plate 1 and Fig. 1 have linear PR wakes. Since spreading rates have remained fairly constant through the past few million years [11], linear wakes imply rapid initiation of propagation followed by constant-rate propagation. In a few areas the direction of propagation reverses abruptly leaving behind a 'W' signature in the gravity field which is characteristic of a 'dueling propagator' [12]. These 'W' patterns occur in areas where the along-axis gradient of the gravity field is either small or differs in sense between long-wavelength and segment-scale trends.

(3) Where there is a pronounced along-axis gravity gradient (Plate 1 and Table 1) or seafloor bathymetry gradient (Table 2), PRs propagate down this gradient. To further demonstrate this correlation, we averaged the gravity anomaly within a ~10 km along-axis and ~80 km across-axis window around the ridge to minimize the local gravity anomalies associated with ridge-axis morphology. This smoothed ridge-axis anomaly is plotted versus distance along the ridge for each of the four areas shown in Fig. 1; PRs are numbered and their directions of propagation are indicated. The direction of ridge propagation is strongly correlated with this measure of the along-axis gradient. Along the Southeast Indian Ridge (Fig. 1a), nine of eleven PRs propagate downhill. The only place where the propagation direction is *not* down the regional gradient is for #3 (a dueling propagator which is migrating down the local along-axis gradient) and #4 (another dueling propagator). Since the 'along-axis gradi-

ent' that we plot is an ~ 80 km wide average of the across-axis gravity, it is likely that both #3 and #4 have a large off-axis component to this gravity measure from the large relief associated with the off-axis 'W' signature of these features. The correlation is equally striking for the Pacific–Antarctic Ridge (#12–#14), and Chile Rise (#21–#22) where five of six PRs propagate downhill. (Note that the along-axis gradient for the wrong-sense PR #23 is dominated by the off-axis high associated with the transverse ridge of a nearby large transform.) The correlation for the Southern Mid-Atlantic Ridge is somewhat less striking, although eight of these eleven PRs appear to propagate downhill and no PR appears to propagate uphill. This lesser correlation is due to both the existence of less-well-developed along-ridge gravity gradients, and the greater 'noise' due to greater tectonic relief near transform faults. (For this ridge we need to average the gravity anomaly within a ~ 20 km along-axis and ~ 140 km across-axis window to smooth the along-axis gravity to a level that is comparable to that of the other figures.) However, even here, wherever there is a pronounced along-axis gradient, PRs are seen to propagate down this gradient (e.g., #24,#26–#29). The correlation between propagation direction and along-axis topographic gradient has been noted in other areas. For example, at the Cocos–Nazca spreading center PRs propagate away from the along-axis high caused by the Galapagos Hotspot in both easterly and westerly directions. In summary, these results strongly support prior claims that where there is a pronounced along-axis bathymetry gradient, PRs will propagate in the downhill direction of this gradient [13,14].

(4) There is a major difference between PRs whose growing segment is an axial high and PRs whose growing segment is a median valley (Fig. 2). (The retreating segment may be a median valley without any apparent change in 'axial high' systematics.) Axial high PRs propagate at roughly 50–150% of their ridge spreading rate and leave behind an asymmetric wake. The outer pseudofault appears as a continuous linear trough or step while the sheared zone appears as a chain of small gravity bumps (Fig. 2) that is sometimes difficult to trace. In a few cases the outer pseudofault scar does not appear while there is a prominent expression of the sheared zone. Below, we propose that the absence of an outer pseudofault signature implies a small age offset between the propagating and dying ridges.

The asymmetry in the PR wake enables one to establish the direction of offset of paleo-PRs. For example, two prominent paleo-PR wakes are seen on the flanks of the Southeast Indian Ridge (Fig. 1a) at 85°E and 93°E. The outermost (oldest) PR was propagating toward the east; this was followed by an episode of westward propagation. Based on our asymmetry observation we note that both the paleo-PRs had right-lateral offsets.

In contrast to the axial high PRs, the median valley PRs propagate at only ~ 15–30% of their spreading rate and have prominent linear troughs along both the outer pseudofault and sheared zone. These median valley PRs are best seen along the Southern Mid-Atlantic Ridge [5]. Along the Southeast Indian Ridge both PR types are

Fig. 1. Gravity curvature maps for selected study regions in Plate 1. All regions are shown in an oblique Mercator projection about the pole of relative motion for the two plates which bound the spreading center. Poles of relative motion from NUVEL-1 [11]. In this projection ridge segments roughly lie along lines of latitude and transform faults lie along lines of longitude. For each panel a colocated inset panel shows ridge geometry and location of propagating ridges (PRs) found in this study. PR numbers correspond to numbers in Table 1. At the bottom of each figure is a profile of the smoothed gravity field along the ridge axis, with '>' symbols showing the direction of propagation and location of each PR tip. (a) Region bounded by latitude–longitude corners at (60°S,75°E) and (35°S,150°E). This region includes the Southeast Indian Ridge west and east of the Australian–Antarctic Discordance. (b) Region bounded by latitude–longitude corners at (65°S,180°E) and (55°S,220°E). This region includes the Pacific–Antarctic spreading center. (c) Region bounded by latitude–longitude corners at (50°S,255°E) and (30°S,290°E). This region includes the Chile Rise. (d) Region bounded by latitude–longitude corners at (52°S,330°E) and (30°S,0°E). This region includes the Southern Mid-Atlantic Ridge.

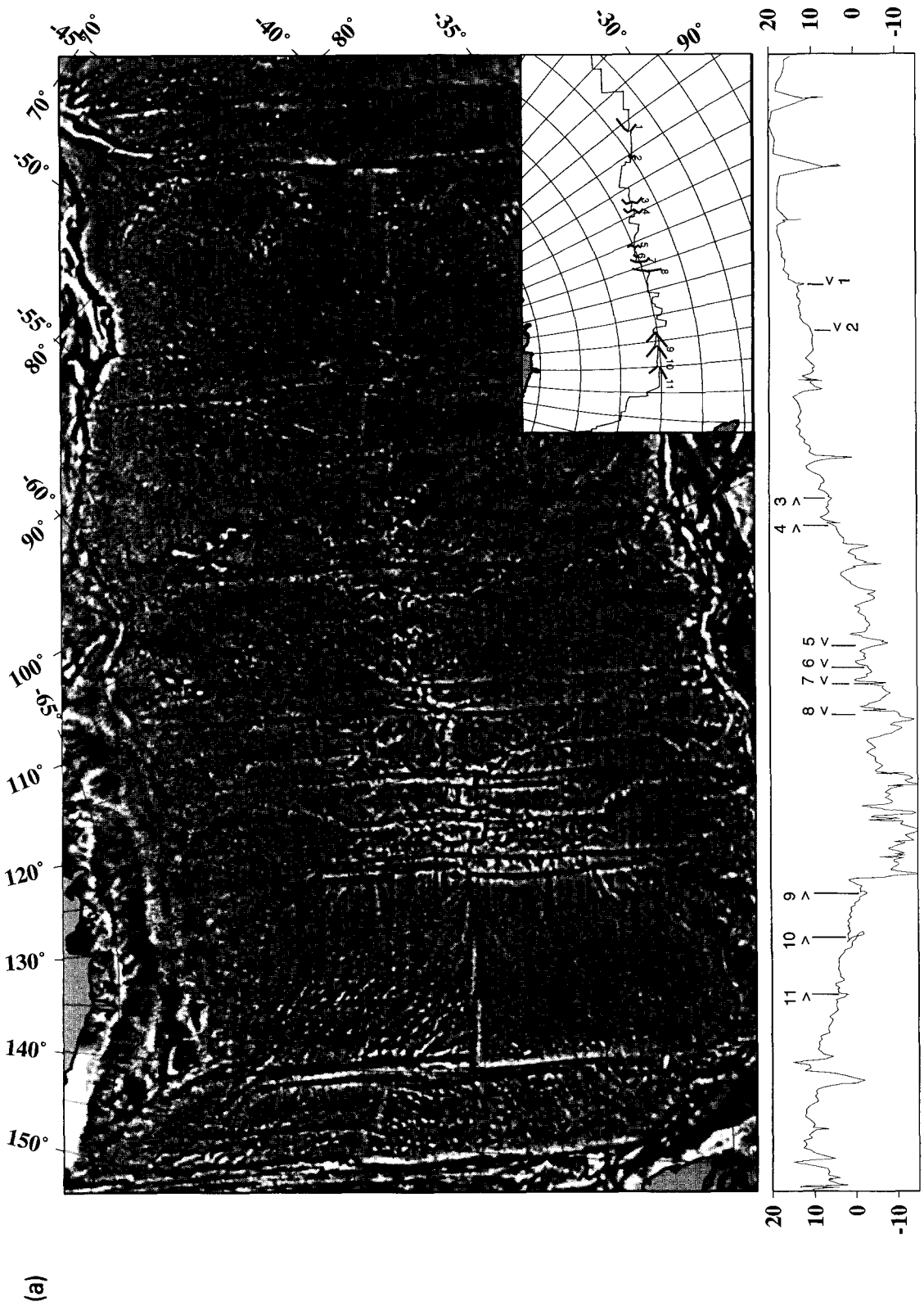
-45°
-40°
-35°
-30°
70°
-50°
-55°
80°
-60°
90°
100°
-65°
110°
120°
130°
140°
150°
20
10
0
-10
V 1
V 2
4 3
8 7 6 5
11
10
9
(a)

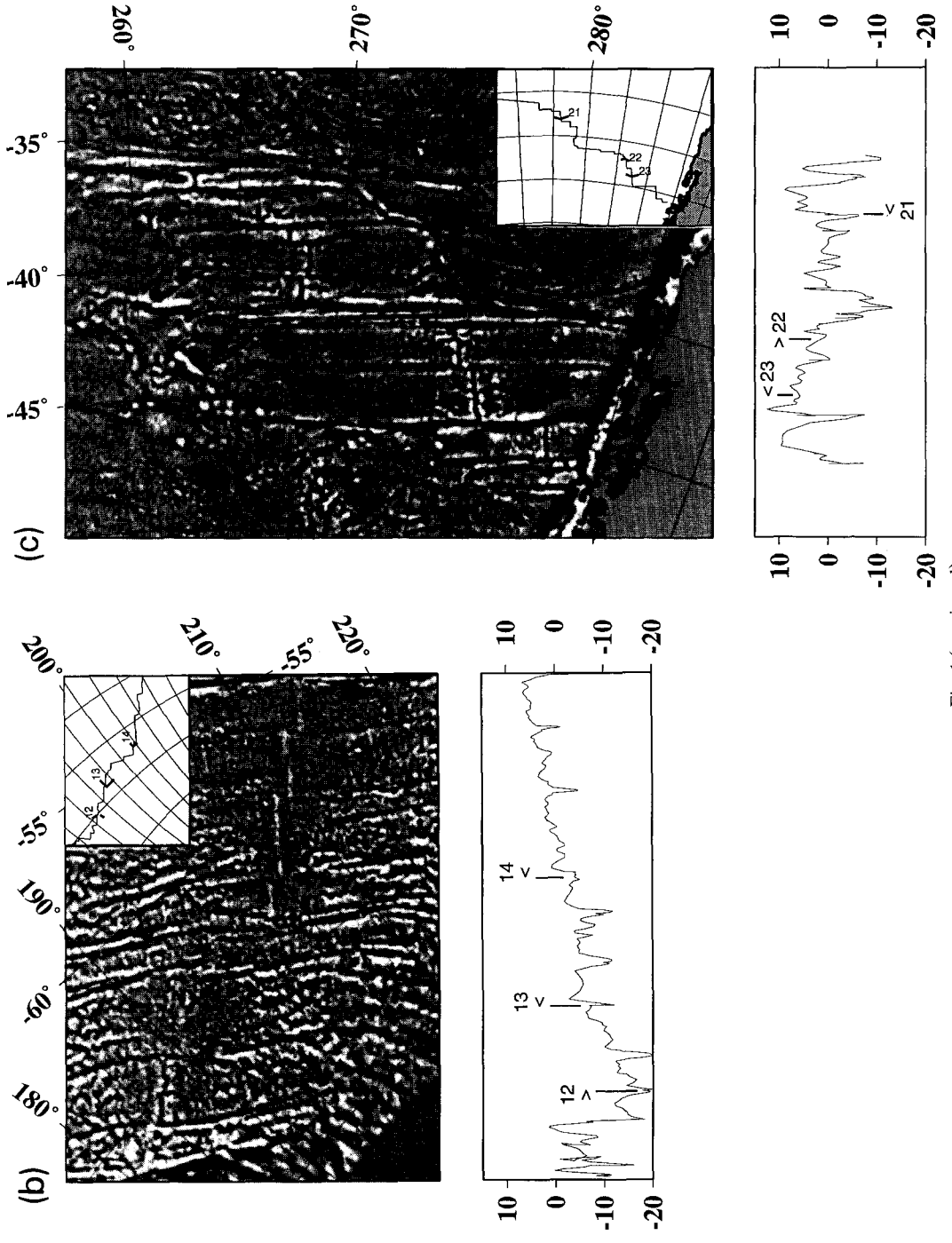

Fig. 1 (continued).

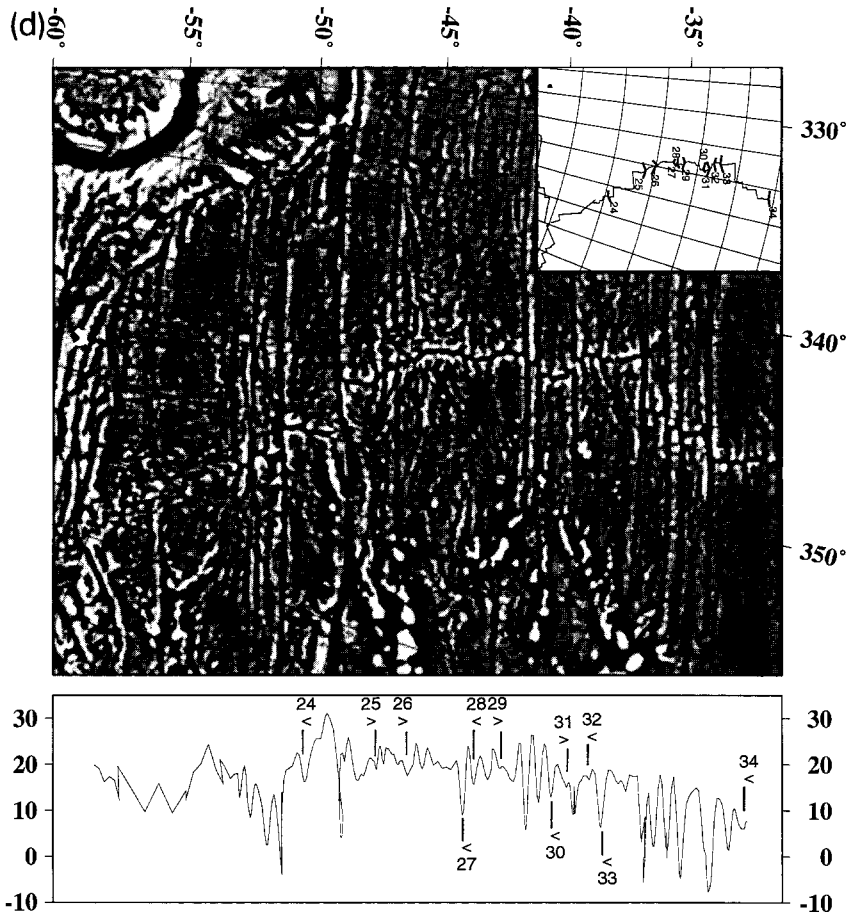

Fig. 1 (continued).

present (e.g., axial high #1,#9–#11; median valley #4–#8).

(5) Finally, the direction of offset of a PR is correlated with recent changes in spreading direction. For example, along the Southeast Indian Ridge where there has been a recent clockwise change in spreading direction [S. Cande, pers. commun.] all the PRs have a right-lateral offset. This sense of offset helps to keep the present spreading ridge perpendicular to the present spreading direction. PRs east of the discordant zone (127°E–138°E) all propagate downhill toward the west; they appear to spawn at the major transform fault at 138°E and become annihilated at the major transform bounding the Australian–Antarctic Discordance (AAD) (127°E). Most PRs to the west of the discordant zone are propagating downhill toward the east yet they have right-lateral offsets. For the past 5 m.y., while the spreading direction has been changing, a continuous series of PRs has apparently resulted in overall asymmetric spreading with apparent faster spreading towards the south (see discussion below). However it is striking that the neighboring Southeast Indian Ridge to the east (141°E–147°E) has had a clear history of propagation transferring lithosphere to the northern Indian Plate.

There is the opposite sense of offset for PRs propagating north and south along the Mid-Atlantic Ridge. Here, pairs of PRs may propagate north and south away from a common mid-segment high (e.g., #28–#29; #30–#31). This

pattern of propagation leads to asymmetric spreading with faster spreading to the west, which tends to keep the ridge axis closer to neighboring hotspots to the east.

3. The relationship between propagation rate and wake morphology

Based on these observations, we speculate that the speed of ridge propagation, and resulting PR structures, are controlled by the strength and the thermal structure of the lithosphere that is rifted by the growing ridge. Median valley PRs, seen at slower spreading ridges, propagate at $\sim 25\%$ of their spreading rate while the axial high PRs seen at intermediate-spreading ridges propagate at $> \sim 50\%$ of their spreading rate. Cormier and Macdonald have recently shown that, at the fast-spreading East Pacific Rise between 18° and 19°S, individual migrating OSCs can migrate extremely rapidly, leaving a (very subdued) wake that differs by only 2–3° from the ridge azimuth [15]. At slower spreading rates, both the sheared zone

Table 1
Characteristics of active propagating ridges south of 30°S

#	Location (lat,lon)	Q[1]	PR Dir.	Off.[2]	Sp.Rate[3] (mag,az)	PR Rate[4]	PR/SR[5]	Down?[6]	PR Start	Comments [references] We show only Geosat results.
Southeast Indian Ridge										
1.	-43.5, 91.8	G	ESE	RL	73,36	48	0.66	D	Transform	Axial High, Crosses Transform
2.	-45.1, 95.8	P	ESE		74,33	36	0.48	D	Transform	
3.	-47.8, 102.8	F	WNW		75,27	18	0.24	N	Middle	Median Valley, dueling PR
4.	-48.0, 104.1	F	WNW		75,26	22	0.29	U	?	Median Valley, dueling PR
5.	-49.8, 111.0	G	ESE	RL	75,22	22	0.29	D	Middle	Median Valley, dueling PR
6.	-50.2, 112.8	F	ESE		75,21	34	0.45	D	Middle	
7.	-50.2, 114.0	P	ESE	RL?	75,20	22	0.29	D		Median Valley, stopped?
8.	-50.2, 115.7	F	ESE	RL	75,18	7	0.10	D	?	Big Valley, stopped at transform
9.	-50.2, 128.3	G	W	RL	74,9	40	0.54	D	Transform	Axial High [2, 4]
10.	-50.1, 130.9	G	W	RL	74,7	49	0.66	D	Transform	Axial High [2, 4]
11.	-50.2, 135.0	G	W	RL	73,4	43	0.59	D	Transform	Axial High
Pacific-Antarctic Ridge										
12.	-65.1, 186.8	F	ENE	LL	59,-42	12	0.21	D	?	Median Valley, stopped at transform
13.	-63.7, 192.7	G	WSW	LL	63,-46	38	0.61	D	Transform	Axial High
14.	-62.2, 204.2	P	WSW	LL?	69,-53	26	0.38	D	Transform	Axial High?, Small offset
15.	-58.9, 211.0	G	?	RL	75,-58					Overlapping Spreading Center(*OSC*)
16.	-53.0, 242.0	G	?	RL	87,-74					*OSC* [6]
17.	-50.8, 242.6	P	?	LL	89,-74					*OSC* [6]
18.	-48.4, 246.6	P	?	RL	92,-76					*OSC* [6]
19.	-41.4, 248.7	P	?	RL	96,-78					*OSC* [6]
20.	-36.3, 249.3	P	?	RL	99,-78					*OSC* [6]
Chile Rise										
21.	-38.1, 266.0	F	S	RL	59,89	12	0.21	D	Middle	Median Valley [24]
22.	-42.0, 276.1	P	N	RL	60,81	11	0.18	D		Median Valley [24]
23.	-43.9, 277.6	F	S	RL	60,80	13	0.22	U?	Middle	Median Valley [24]
Mid-Atlantic Ridge										
24.	-49.7, 352.0	F	S	LL	33,255	7	0.22	D	Middle	Median Valley
25.	-46.1, 346.0	P	N	RL	34,258	7	0.20	N	Middle	Median Valley
26.	-45.1, 344.7	F	N	RL	34,258	13	0.38	D	Transform	Median Valley, OPF High
27.	-43.0, 343.8	F	S	LL	34,258	10	0.29	D?	Middle	Median Valley
28.	-42.5, 343.9	F	S	LL	34,258	9	0.28	D	Middle	Median Valley
29.	-41.6, 343.4	F	N	RL	34,259	8	0.23	D	Middle	Median Valley
30.	-39.3, 344.0	P	S	LL	35,259	9	0.24	D	Middle	Median Valley
31.	-38.5, 343.7	F	N	RL	35,260	8	0.23	D	Middle	Median Valley
32.	-38.1, 342.7	G	S	RL	35,260	3	0.08	N	Middle	Median Valley
33.	-37.3, 342.7	G	S	LL	35,260	6	0.16	N	?	Median Valley
34.	-30.6, 346.3	P	S	RL	36,258	4	0.11	D		Median Valley [5]

[1] Quality (*G*ood, *F*air, *P*oor); [2] offset (*R*ight *L*ateral, *L*eft *L*ateral); [3] spreading rate (mm/yr, NUVEL-1 [11]) and spreading azimuth (degrees clockwise from north); [4] propagation rate (mm/yr) (this is determined from the angle enclosed by pair of PR wakes (e.g., $V_{PROP} = V_{SPR}/[2\tan\{(\theta_{wake1-wake2})/2\}]$), or, when only one side of a PR wake is seen in the data, from the half-angle between a single PR wake and ridge axis (e.g., $V_{PROP} = V_{SPR}/[2\tan\{\theta_{wake1-axis}\}]$); [5] ratio of propagation rate to spreading rate; [6] propagates *D*own or *U*p regional along-ridge gravity gradient or there is *N*o discernible along-ridge gravity gradient. (The sense of the along-axis gravity gradient is shown in Fig. 1, which was used in conjunction with figures such as Plate 1 to make these determinations.)

and outer pseudofault wakes are characterized by valley signatures. At intermediate rates, the PR wakes are asymmetric as discussed above and the outer pseudofault wake is sometimes absent. Finally, above 75 mm/yr migrating OSCs [6] have such a subdued morphologic expression that they do not produce significant gravity signatures.

We propose that at slow- and intermediate-spreading centers the propagation rate is limited by the time needed to create a 'ridge-hot' spreading segment. The PR tip initially spreads as much colder, stronger lithosphere resulting in a prominent rift tip depression which is transferred to both the sheared zone and outer pseudofault. This origin is a corollary of the hypothesis that median valley relief is created by the extension of strong axial lithosphere [16–19]. At intermediate rates, where the growing ridge has an axial high, the lithosphere is weaker and provides less resistance to the propagation-tip stresses (see next section) so the ratio of propagation rate to spreading rate increases. We speculate that the gravity signature of the outer pseudofault depends on the amplitude of the rift-tip depression which in turn depends on the strength of the lithosphere being rifted. Thus, a larger-offset PR will rift older stronger lithosphere, resulting in a more prominent outer pseudofault. (Note that we no longer favor the hypothesis proposed in [14] that subaxial asthenospheric flow into the growing tip is the origin for the tip depression.) At spreading rates greater than 75 mm/yr, the growing ridge is rifting young and weak lithosphere (unless the offset is large) with little resistance, resulting in a very rapid propagation rate and no significant gravity wake.

4. Dynamics of ridge propagation

Several mechanisms have been proposed to explain the onset and propagation of migrating ridge axis offsets. A fracture mechanics-based model by Phipps Morgan and Parmentier [14] (hereafter PMP) treats ridge segments as cracks in the oceanic lithosphere: the state of stress at a ridge-crack tip is characterized by a stress-intensity factor K, where the stresses near the crack tip asymptotically approach $\sigma_{ij} = KF_i j(\theta)/r^{1/2}$, where r is the radial distance from the tip, θ is the azimuthal angle measured from the crack surface, and the $F_i j(\theta)$ are trigonometric functions of unit magnitude [cf. 20, pp. 53–55]. A ridge will propagate when this stress-intensity factor exceeds a threshold value. In their analysis PMP suggest that gravitational spreading stresses associated with excess ridge topography make a positive contribution K_d to the ridge-tip K which

Table 2
Characteristics of other known active propagating ridges

#	Location (lat,lon)	Q[1]	PR Dir.	Off.[2]	Sp.Rate[3] (mag,az)	PR Rate[4]	PR/SR[5]	Down?[6]	PR Start	Comments [references]
Juan de Fuca Ridge										
35.	48, 231	G	N	RL	61,-62	44	0.72	D	Middle?	'Dueling Propagator' [12, 25, 26]
Cocos-Nazca Ridge										
36.	2.6, 264.5	G	W	RL	58,5	52	0.90	D	?	Axial High. Classic PR. [23, 27-30]
37.	2.5, 267	P	W	LL	55,5	?	?	D	?	Axial High [31]
38.	0.8, 272.8	P	E	RL	64,7	?	?	D	?	Axial High [31]
Easter Microplate										
39.	-25, 247.6	F	N	LL	120,90	150	1.25	D	Middle?	Axial High [9]
40.	-24, 247.9	P	N	LL	?	?	?	D	?	Axial High [10]
41.	-23.5, 248.1	P	N	LL	?	?	?	D	?	Axial High [10]
42.	-26.8, 245.8	P	SE	?	~70,45	100	1.43	D	?	Axial High [10, 32]

See notes beneath Table 1, except for 3, 4 and 5, where the published spreading rate, propagation rate and published ratio of propagation to spreading rate is used (PR #35–36,39,42). (These studies determine the PR rate from fitting local magnetic anomaly picks for the propagating ridge axis and/or fitting the azimuth of the bathymetric expression of the PR wake.) Note 6 refers here to whether or not the propagating ridge propagates *D*own the regional along-ridge gradient in axial bathymetry.

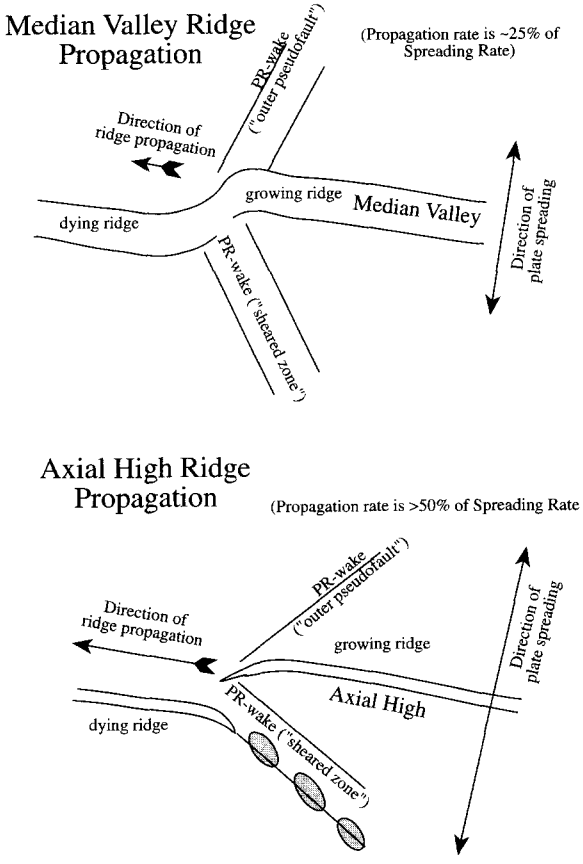

Fig. 2. Cartoon of characteristic geometry of idealized median valley and axial high propagating ridge systems. The Geosat signature of a median valley propagator is a ~ 120° V-shaped valley-flanking high wake. The Geosat signature of an axial high propagator is asymmetric. The outer pseudofault, when present, is a linear trough. The sheared zone usually appears as a chain of oblique hills. The angle of the axial high propagator wake is ~ 90°, i.e. the ratio of the propagation rate to spreading rate is higher than at a median valley propagator. See text for discussion.

favors segment propagation away from a regional along-axis high. The growth of the ridge axis involves the creation of a new spreading center which leads to the transient formation of an axial depression near the propagating ridge tip; this rifting produces a resisting stress-intensity contribution K_r. The dynamic balance between 'far-field' gravitational spreading stresses and propagation-resisting near-tip stresses limits ridge-axis growth to a finite propagation rate.

The observed along-axis bathymetry profile along each of the currently well-mapped active propagating ridges (Galapagos 95.5°W [14], Easter 25°S [14], SEIR 128°E [2] and 131°E [2]) fits this model. (The size of the axial relief anomaly is related to the induced propagation-driving or propagation-resisting horizontal force P by [14]:

$$P = [\sim 0.5 \sim 0.66](\rho_l - \rho_w)\, gH\delta \qquad (1)$$

where H is the axial plate thickness and ρ_l and ρ_w are densities for lithosphere and water respectively. This relation only differs by a factor of 4/3 if the relief is due to viscous instead of isostatic stresses [14].) In general, this hypothesis predicts that PRs will propagate away from broad along-axis highs towards broad along-axis lows. Our results (Fig. 1 and Table 1) support this prediction, if we assume that the regional along-axis gravity reflects regional along-axis bathymetry. While the Geosat data demonstrate the correlation between propagation direction and along-axis gravity gradient, they do not have sufficient resolution to establish the depth of the rift-tip depression. This detailed information is needed for further quantitative modeling [2,14].

It has been proposed that ridge propagation is a consequence of changes in plate motion [13]. In contrast, our new data suggest that a persistent along-axis gradient produces ridge propagation while changes in plate motion determine the offset direction and offset distance of the PR. This is supported by other studies that show evidence for propagation in the absence of significant changes in spreading direction [6,8,21]. A noticeable change in plate motions leads to the rapid growth of the offset at propagating ridges as the new ridge axis forms more nearly perpendicular to the new spreading direction than does the retreating ridge axis. This effect is clearly seen at the 128°E, 131°E and 135°E PRs along the Southeast Indian Ridge. All three PRs show a gravity signal of a northern outer pseudofault wake at roughly the same time (~ 4 Ma), which presumably marks the beginning of a significant change in plate motion. However, the signatures of the sheared zones can be traced on older seafloor to a common origin point at the transform at 138°E suggesting that all three PRs initially propagated

at different times and initially had insufficient offset to produce a detectable outer pseudofault signature. After the recent change in spreading direction, all three have become larger-offset PRs with a wake on both sides of the ridge axis. This example supports the hypothesis that ridge propagation is a mechanism for ridge reorientation in response to a change in plate spreading direction. However, it shows that ridge propagation also occurs in the absence of noticeable changes in plate spreading direction. Finally we note that numerous small-offset PRs could produce a magnetic record that could be easily confused with continuous asymmetric accretion.

It has also been proposed that a ridge will propagate due to the influence of far-field extensional forces on the spreading center; longer cracks will grow at the expense of shorter segments [7]. The unbalanced far-field horizontal stress of $\sigma_{FF} = 30$ MPa that is needed for this model [7] is probably much too large (while far-field stresses are likely to be of this size, unbalanced far-field stresses are not). Evaluating (1) for $H\sigma_{FF} = P$ shows this to be equivalent to gravitational spreading stresses due to 3 km of anomalous along-axis relief, i.e. larger than the effect of the largest hotspot influence on the depth of a mid-ocean ridge. If true, this would imply that the largest segment should always be the one which grows, which contradicts the observation that PRs often initiate near a segment high. (For example, the 138°E transform fault on the Southeast Indian Ridge has been a spawning site for many very short PR segments (#9–11 in Table 1) that then lengthened as they propagated westward.) PMP note that a uniform far-field horizontal stress, if balanced by equal and opposite stresses at the ridge axis, will lead to no preference for a longer crack to grow over a neighboring shorter segment. They also note that the mean far-field stress must be balanced by an equal and opposite mean near-ridge resistance. Any support of far-field stresses by near-ridge drag at the base of the plate would simply result in a smaller effective far-field stress that needs to be balanced by forces transmitted across the spreading center. However, along-axis variations in far-field stress (e.g., near a subduction zone [14]) or along-axis variations in plate-extension-resisting stresses (the strength of the axial lithosphere) can lead to a non-zero stress intensity at the ridge-crack tip which favors propagation [14].

There is a possible small segment–length dependence to the crack-tip stress intensity due to the fact that ridge segments are usually shallowest near their segment center and deepest near their segment ends [14]. This effect should, all other effects being equal, slightly favor the propagation of the longer segment. Local increases in along-axis resistance to plate extension may occur at non-transform offsets, or a ridge with a median valley with cold, strong, axial lithosphere as opposed to an axial high with thin, weak axial lithosphere. The fracture-mechanics ridge-crack theory implies that these lateral strength variations will tend to favor the propagation of a weaker axial high segment to replace a stronger median valley segment. We see some examples on this phenomena, but no examples where this effect appears to overpower the tendency to propagate down an along-axis gravity gradient.

Several examples have been found in the North Pacific where paleo-ridge propagation occurred in a direction which presently is 'uphill' [18,19]. If these examples are robust, we must reconcile the apparent contradictory observation that our present study shows that active propagating systems propagate downhill wherever a pronounced along-axis gradient is seen. A possible reconciliation is that, if paleo-propagators did indeed propagate downhill, much of their along-axis bathymetric gradient was due to a component of dynamic axial relief that subsequently disappeared as the seafloor moved off-axis. This would provide indirect support for the recent hypothesis that there is a significant component of seafloor relief due to pressure gradients associated with asthenosphere flow [22].

5. Ridge propagation and asymmetric plate accretion

Repeated ridge propagation is a mechanism for asymmetric plate accretion [13]. This effect has been recently documented along the East

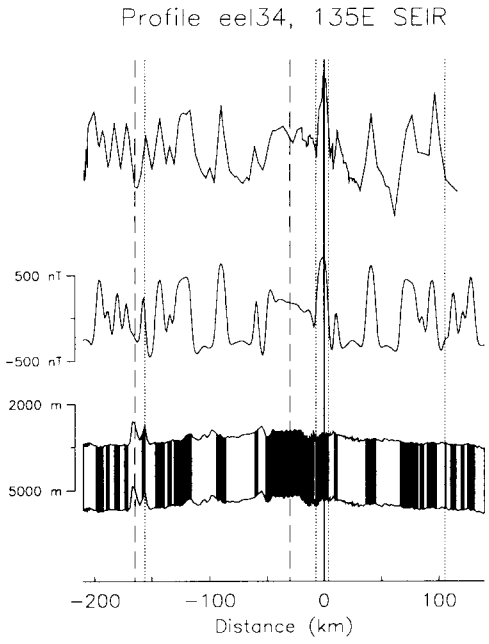

Fig. 3. Magnetic anomaly profile across the Southeast Indian Ridge at 135° (data from Eltanin Leg el134, projected on a N–S line which is the overall strike of this ship profile). (Top) Observed magnetic anomaly near the spreading axis. (Middle) Synthetic magnetic anomaly profiles calculated from observed seafloor bathymetry profile and a calculated seafloor magnetization which includes symmetric spreading at 74 mm/yr from 0 to 2.4 Ma and 66 mm/yr before 2.4 Ma. Synthetics model two episodes of ridge propagation (a 23 km northward ridge jump at 0.15 Ma and an 8.5 km northward ridge jump at 3.67 Ma). (Bottom) Seafloor bathymetry and magnetization used for synthetic calculation in middle panel. Note that while instantaneous spreading is symmetric, pronounced asymmetric accretion occurs due to a consistent northward pattern of ridge jumping associated with westward ridge propagation. Location of current axis of spreading is shown by a heavy vertical line. Locations of seafloor moved by past ridge propagation events are shown by vertical dashed lines.

Pacific Rise between 18° and 19°S [15], and is clearly seen along the Southeast Indian Ridge east of 127°E. Fig. 3 shows a N–S magnetic profile which crosses the currently active PR at 135°E (#11 in Table 1). This profile has asymmetric overall accretion that is faster to the south. This pattern is consistent with the numerous PR sheared zone wakes on the southern flank of the Southeast Indian Ridge between 127° and 138°E in Plate 1 and Fig. 1a. Fig. 3 also shows a synthetic magnetic anomaly pattern due to symmetric spreading with small ridge jumps at the sites marked by dashed lines. Noticeable jumps in the magnetic record are found at the major southern topographic bumps 160, 225 and 340 km south of the current spreading axis. The locations of these bumps correlate well with the locations where notable near-ridge PR sheared zone wakes cross the 135°E meridian in Fig. 1, evidence which further suggests that ridge propagation is the key process causing systematic asymmetric spreading at this ridge.

This new data suggests that systematic ridge propagation in a preferred direction can lead to overall asymmetric accretion, accretion whose sense is related to the direction of ridge propagation and the overall orientation of the spreading segment with respect to the spreading direction [13,23]. This mechanism could lead to the growth (or elimination) of a transform offset where propagators 'die' as they produce an increase (or decrease) in the length of this transform fault. It could also lead to transform fault growth that depends on whether PRs nucleate from a transform with little change in transform length, or die at a transform after they have accumulated a significant ridge offset during their previous propagation history.

This mechanism for asymmetric accretion seems straightforward until we consider the evolution of the neighboring Southeast Indian Ridge between 141° and 147°E. This segment has numerous PR sheared zone wakes to the northern side of the ridge. This is curious. Changes in ridge azimuth in response to changes in plate motion should result in a similar sense of ridge offset for propagation in the same direction unless the original ridge azimuths are quite different. It is clear that overall ridge azimuths between 127–138°E and 141–147°E are different by ~ 12° (Fig. 1a). However, both have experienced frequent episodes of propagation which, in general, is thought to reorient a ridge perpendicular to a new spreading direction. For one PR episode, this would work fine, but after this episode both segments should have the same azimuth and subsequent PR episodes in the same direction should put sheared zone offsets on the same flank of the ridge. Possibly an oblique, weak ridge leads to a

reorientation of local tensile stress field to a direction between the ridge azimuth and far-field plate extension direction so that propagation moves the new spreading axis toward, but not to, a spreading-perpendicular direction so that an initially oblique ridge will only slowly rotate into a new direction. It is also possible that the spreading center between 141° and 147°E experiences a permanent rotation of the principle local tensile stress away from the spreading direction, due to stress-couple of the two long-offset left-lateral transform faults which bound this macrosegment. We need better constraints on the evolution and morphology of this ridge to be able to test whether any of these ideas offers any promise for explaining this enigmatic accretion history.

High-resolution Geosat data has allowed us to answer several first-order questions about the causes and consequences of ridge propagation. However, to answer many of the questions that this study raises will require detailed bathymetric and magnetic studies at several of these newly located propagating ridges and long-profile magnetic and bathymetric surveys of the history of asymmetric accretion along specific spreading segments.

6. Acknowledgements

We thank Ken Macdonald and two anonymous reviewers for helpful comments. Dick Hey and Dave Caress provided the MAGBATH program used to do the synthetic magnetic anomaly modeling in Fig. 3 (Dick Hey also introduced JPM to geophysical research by hiring him to write the initial version of this program. This opportunity is gratefully acknowledged.) This work was partially supported by the National Science Foundation.

7. References

[1] D.T. Sandwell and W.H.F. Smith, Global marine gravity from ERS-1, Geosat, and Seasat reveals new tectonic fabric, EOS Trans. AGU 73, 133, 1992.

[2] J. Phipps Morgan et al., Propagating rifts along the Southeast Indian Ridge, EOS Trans. AGU 69, 1430, 1988.

[3] J. Palmer et al., Morphology and tectonics of the Australian–Antarctic Discordance, Mar. Geophys. Res. 15, 121–152, 1992.

[4] P.R. Vogt, N.Z. Cherkis and G.A. Morgan, Project Investigator-I: Evolution of the Australia–Antarctic Discordance from a detailed aeromagnetic study, in: Antarctic Earth Science, Proceedings of the 4th International Symposium on Antarctic Earth Science, R.L. Oliver et al., Aust. Acad. Sci., 1984.

[5] S. Carbotte, S.M. Welch and K.C. Macdonald, Spreading rates, rift propagation and fracture zone offset histories during the past 5 my on the Mid-Atlantic Ridge: 25°–27°30′S and 31°–34°S, Mar. Geophys. Res. 13, 51–80, 1991.

[6] P. Lonsdale, Geomorphology and structural segmentation of the crest of the Southern (Pacific–Antarctic) East Pacific Rise, J. Geophys. Res., submitted, 1993.

[7] K.C. Macdonald, D.S. Scheirer and S.M. Carbotte, Mid-ocean ridges: Discontinuities, segments, and giant cracks, Science 253, 986–994, 1991.

[8] K.C. Macdonald, J.C. Sempéré and P.J. Fox, East Pacific Rise from Siqueiros to Orozco fracture zones: along-strike continuity of axial neovolcanic zone and structure and evolution of overlapping spreading centers, J. Geophys. Res. 89, 6049–6069, 1984.

[9] D.F. Naar and R.N. Hey, Fast rift propagation along the East Pacific Rise near Easter Island, J. Geophys. Res. 91, 3425–3438, 1986.

[10] D.F. Naar and R.N. Hey, Tectonic evolution of the Easter Microplate, J. Geophys. Res. 96, 7961–7993, 1991.

[11] C. DeMets et al., Current Plate Motions, Geophys. J. Int. 101, 425–478, 1990.

[12] H.P. Johnson et al., A detailed study of the Cobb offset of the Juan de Fuca ridge: Evolution of a propagating rift, J. Geophys. Res. 88, 2297–2315, 1983.

[13] R. Hey, F.K. Duennebier and W.J. Morgan, Propagating rifts on midocean ridges, J. Geophys. Res. 85, 3647–3658, 1980.

[14] J. Phipps Morgan and E.M. Parmentier, Causes and rate-limiting mechanisms of ridge propagation: a fracture mechanics model, J. Geophys. Res. 90, 8603–8612, 1985.

[15] M.-H. Cormier and K.C. Macdonald, East Pacific Rise 18°–19°S: Asymmetric spreading and ridge reorientation by ultra-fast migration of axial discontinuities, J. Geophys. Res., submitted, 1993.

[16] P. Tapponier and J. Francheteau, Necking of the lithosphere and the mechanics of slowly accreting plate boundaries, J. Geophys. Res. 83, 3955–3970, 1978.

[17] J. Phipps Morgan, E.M. Parmentier and J. Lin, Mechanisms for the origin of mid-ocean ridge axial topography: Implications for the thermal and mechanical structure at accreting plate boundaries, J. Geophys. Res. 92, 12823–12836, 1987.

[18] Y. Chen and W.J. Morgan, A nonlinear-rheology model for mid-ocean ridge axis topography, J. Geophys. Res. 95, 17583–17604, 1990.

[19] J. Phipps Morgan and Y.J. Chen, The genesis of oceanic crust: Magma injection, hydrothermal circulation, and crustal flow, J. Geophys. Res. 98, 6283–6298, 1993.

[20] B.R. Lawn and T.R. Wilshaw, Fracture of Brittle Solids, Cambridge University Press, 1975.

[21] K.C. Macdonald et al., Deep-tow and Sea Beam studies of dueling propagating ridges on the East Pacific Rise near 20°40'S, J. Geophys. Res. 93, 2875–2898, 1988.

[22] J. Phipps Morgan and W.H.F. Smith, Flattening of the seafloor depth–age curve as a response to asthenospheric flow, Nature 359, 524–527, 1992.

[23] R.N. Hey et al., Sea Beam/Deep-Tow investigation of an active oceanic propagating rift system, Galapagos 95.5°W, J. Geophys. Res. 91, 3369–3393, 1986.

[24] L. Kovacs et al., An aeromagnetic survey of the Chile Ridge, part I: A tectonic overview, EOS Trans. AGU 71, 621, 1990.

[25] D.S. Wilson, R.N. Hey and C. Nishimura, Propagation as a mechanism of reorientation of the Juan de Fuca ridge, J. Geophys. Res. 89, 9215–9225, 1984.

[26] J.L. Karsten and J.R. Delaney, Hot spot–ridge crest convergence in the Northeast Pacific, J. Geophys. Res. 94, 700–712, 1989.

[27] M.C. Kleinrock and R.N. Hey, Detailed tectonics near the tip of the Galapgos 95.5°W propagator: How the lithosphere tears and a spreading axis develops, J. Geophys. Res. 94, 13801–13838, 1989a.

[28] M.C. Kleinrock, R.C. Searle and R.N. Hey, Tectonics of the failing spreading center associated with the 95.5°W propagator, J. Geophys. Res. 94, 13839–13858, 1989b.

[29] M.C. Kleinrock and R.N. Hey, Migrating transform zone and lithospheric transfer at the Galapagos 95.5°W Propagator, J. Geophys. Res. 94, 13859–13878, 1989c.

[30] J. Phipps Morgan and M.C. Kleinrock, Transform zone migration: Implications of bookshelf faulting at oceanic and Icelandic propagating ridges, Tectonics 10, 920–935, 1991.

[31] D.M. Christie and J.M. Sinton, Evolution of abyssal lavas along propagating segments of the Galapagos spreading center, Earth Planet. Sci. Lett. 37, 321–325, 1981.

[32] R.N. Hey et al., Microplate tectonics along a superfast seafloor spreading system near Easter Island, Nature 317, 320–325, 1985.